Proceedings of the 18th World Congress
The International Federation of Automatic Control
Milano (Italy) August 28 - September 2, 2011

Robust High Fidelity Needle Insertion in Soft Tissues Implemented on a Teleoperation System

M.R. Dehghan* S.M. Rezaei* H.A Talebi M.Zareinejad*****

** Mechanical Engineering Department, Amirkabir University of Technology, Tehran, Iran, (e-mail: {mr_dehghan, smrezaie} @aut.ac.ir).*
*** Electrical Engineering Department, Amirkabir University of Technology, Tehran, Iran, (e-mail: alit@aut.ac.ir)*
**** New Technologies Research Centre (NTRC), Amirkabir University of Technology, Tehran, Iran, (e-mail: mzare@aut.ac.ir)*

Abstract: Robot-assisted needle insertion has attracted considerable attention in recent years, due to its application in minimally invasive percutaneous procedures. The main goal of teleoperated needle insertion is accurate tracking of needle in free motion and during insertion. In this research a 1-DOF master/slave needle insertion is introduced. The uncertain dynamics of the slave robot has been considered through the teleoperation loop. An impedance controller has been used for master side and a sliding-mode-based impedance controller is proposed for the slave robot to compensate its uncertain dynamics. Robust control architecture was used to optimize the fidelity measure with constraints on the free motion tracking requirements and robust stability of the system under uncertainties of the soft environment. The validity of the proposed control scheme is demonstrated by experiments with a teleoperation needle insertion set-up. Experimental results indicated effectiveness of this controller to achieve precise tracking during contact and free motion.

Keywords: Teleoperation needle insertion, Robust control, Fidelity, Sliding mode control, Impedance control.

1. INTRODUCTION

Robot-assisted needle insertion has attracted considerable attention in recent years, due to its applications in minimally invasive percutaneous procedures such as biopsy and brachytherapy (Abolhassani et al. 2007). In robotic needle insertion, a robot is used to control the position and orientation of the base of a stiff symmetric needle to guide the tip of the needle to a desired target inside the tissue (Mahvash et al. 2010). In these procedures, needles are used, for example, to place radioactive seeds at tumor sites, to extract biopsy samples, and to inject drugs; therefore accurate tracking of the needle shaft inside the soft tissue is of fore most importance. The main goal of teleoperated needle insertion is accurate tracking of needle in free motion and during insertion. Moreover, availability of force feedback for the operator will improve the success rate of the needle insertion task (Abolhassani et al. 2009).

In telesurgery, ideal goal is that surgical operations to be performed by teleoperator controlled by surgeons from a remote location via the Internet. Surgeons depend primarily on their haptic sense to detect target tissues. So it is of great importance for the teleoperator to transmit the dynamics of the remote environment to the human operator reliably and accurately. The fidelity function is appropriate for the applications such as telesurgery, where the ability to recognize small changes in tissue compliance is essential for tasks such as tumor detection or detection of embedded vessels (Cavusoglu et al. 2002). The main benefit of master–slave needle insertion is that the surgical tool can be controlled by the surgeon remotely; therefore the surgeon's expertise is in the loop (Abolhassani et al. 2009). In teleoperation with hard environment, the main problem is to maintain stability during the maneuver since contact between the robot arms and the stiff environment can easily cause unstable situations. However, in applications that involve manipulation of soft objects, like telesurgery, the feedback fidelity of contact force between the manipulator and remote soft object become a critical concern which must be considered in addition to stability considerations.

Abolhassani et al. (2009) have performed a teleoperated needle insertion in a pig's heart. The effect of force feedback on the accuracy of needle insertion has been studied and it has been shown that incorporation of force feedback can improve teleoperated needle insertion. Unfortunately, their approach has not focused on force/position tracking issues during insertion. Cavusoglu et al. (2002) designed a controller to improve telemanipulation performance in soft environment. They defined the fidelity as a measure of sensitivity of the transmitted impedance to changes in the environmental impedance. Wang et al. (2005) designed a robust controller scheme to improve fidelity in soft environment. They proposed the fidelity measure as the difference between the transmitted impedance and the environmental impedance. In both studies, they have designed a robust controller to environment and human uncertainty, but they have not considered any uncertainty on

master/slave robot dynamics. Also they have not considered scaling factors in their fidelity measure. Buttolo et al. (1994) proposed a sliding mode controller for both master and slave to overcome their uncertainties. Cho and Park (2005) implemented an impedance control for the master and a modified sliding mode control for the slave. Their controllers were designed for a wide range of environment impedance which is a conservative condition that weakens the transparency. Furthermore, their controller does not provide an admissible position tracking when the slave robot is in contact with the environment.

In this research the uncertainties of the slave and the environment were taken into account separately. At the master side an impedance controller was utilized as proposed by Cho and Park (2005). To cope with the uncertainty at the slave side, an impedance model was put into a sliding surface of a sliding-mode based controller. At the same time, this controller injects desired impedance to the slave robot. Soft tissue has been assumed to be inhomogeneous, nonlinear, anisotropic and elastic. An impedance range was considered for soft tissue and a robust controller was proposed to overcome environment uncertainty which is a modification to the controller introduced by Cavusoglu et al. (2002). This controller stabilizes the linear dynamics resulted from previous step. It is formulated as the optimization of fidelity measure with constraints on the free motion tracking requirements and robust stability of the system under environment uncertainties. The proposed controllers guarantee teleoperator stability in free motion and during insertion.

2. MASTER AND SLAVE DYNAMIC MODELING

In this research, the master manipulator, a DC servo-motor, has one degree of freedom. The dynamics of the motor is modeled with a mass-spring-damper system.

$$j_m\ddot{\theta}_m + b_m\dot{\theta}_m + k_m\theta_m = u_m + f_h.L_{eff}. \quad (1)$$

where θ_m denote the angular position of DC motor and j_m, b_m and k_m are the moments of inertia of the rotating system, damping and stiffness, respectively; f_h denotes the force applied at the master side by the operator, L_{eff} is the effective length between the force and motor shaft, and u_m is the master control signal.

The slave robot used for studying needle insertion in soft tissue was a linear actuator. The manipulator provided needle motion with one degree of freedom, translation in one (horizontal) direction. Dynamic model of the linear motor can be considered as follows

$$m_s\ddot{x}_s + b_s\dot{x}_s + k_s x_s = u_s - f_e. \quad (2)$$

where x_s is the slave position and m_s, b_s and k_s are mass, viscous damping coefficient and stiffness, respectively; u_s denotes the slave control signal and f_e is the force exerted by the environment to the slave.

Position, velocity and acceleration of the master, and contact force from the slave can be scaled according to the application.

$$\begin{cases} x_s = k_p\,\theta_m \\ f_h = k_f\,f_e \end{cases} \quad (3)$$

where k_p and k_f are position and force scale factors, respectively.

3. CONTROLLER DESIGN

The main objective of impedance control is maintaining a desired dynamic relationship between robot position and contact force. An impedance controller and a sliding-mode based impedance controller are designed for the master and the slave, respectively. Resulting linear dynamics will be used in the next section where a robust controller guarantees the stability and high fidelity performance of the total telemanipulation system.

3.1 Impedance Control for the Master

The force based impedance control on the master side reflects the contact forces to operator. With an impedance control, a desired dynamic behavior between human operator and master device can be realized. The desired impedance equation for master is specified such that

$$\bar{j}_m\ddot{\theta}_m + \bar{b}_m\dot{\theta}_m + \bar{k}_m\theta_m = (f_h - k_f\,f_e)L_{eff}. \quad (4)$$

where $\bar{j}_m$, $\bar{b}_m$, and $\bar{k}_m$ are the desired inertia, viscous damping coefficient, and stiffness, respectively. Combining (4) and (1) to remove acceleration, $\ddot{\theta}_m$, results to the master control input as

$$u_m = \left[b_m - \frac{j_m}{\bar{j}_m}\bar{b}_m\right]\dot{\theta}_m + \left[k_m - \frac{j_m}{\bar{j}_m}\bar{k}_m\right]\theta_m + \left[\frac{j_m}{\bar{j}_m} - 1\right]f_h\,L_{eff} - \frac{j_m}{\bar{j}_m}k_f\,f_e\,L_{eff}. \quad (5)$$

3.2 Sliding-mode-based impedance controller for the slave

In slave control, tracking performance in the free motion and contact stability of the slave depends to the desired impedance model. A desired impedance equation for the slave is as follows

$$\bar{m}_s\ddot{x}_s + \bar{b}_s\dot{x}_s + \bar{k}_s x_s = \alpha f_e - p(x_s - k_p\,x_m) - f_e. \quad (6)$$

where p and α are two control parameters that will be chosen to guarantee stability and transparency in next section. In (6) $\bar{m}_s$, $\bar{b}_s$, and $\bar{k}_s$ are the desired inertia, viscous damping coefficient, and stiffness, respectively. To deal with parametric uncertainties, unmodeled dynamics and identification error, a robust impedance controller can be achieved by designing a sliding-mode controller such that the desired impedance model becomes exact on the sliding surface. This sliding-mode based impedance control, originally proposed for force regulation by Lu et al. (1995), uses a robust property of a sliding control against uncertainties. Sliding surface, $s(t)$, was defined as

$$s(t) = \frac{1}{\bar{m}_s}\int_0^t I(\tau)\,d\tau \quad (7)$$

where I(t) is the difference between both sides of the desired impedance equation.

$$I(t) = \bar{m}_s\ddot{x}_s + \bar{b}_s\dot{x}_s + \bar{k}_s x_s + p\left(x_s - k_p\,\theta_m\right) + (1-\alpha)f_e \quad (8)$$

The desired impedance characteristic can be obtained only when $I(t)$ is converged to zero. If the sliding condition of $s(t).\dot{s}(t) \le -\eta.|s(t)|$ is satisfied, the system trajectories point toward the sliding surface, $s(t)$, where η is a strictly positive constant and specify the minimum speed for states to reach the sliding surface (Slotine and Li 1991).

Solving $\dot{s}(t) = 0$, the control input to the slave was obtained as

$$u_s = f_e + \hat{b}_s\dot{x}_s + \hat{k}_s x_s - \frac{\hat{m}_s}{\bar{m}_s}\left[\bar{b}_s\dot{x}_s + \bar{k}_s x_s + p\left(x_s - k_p\,\theta_m\right) + (1-\alpha)f_e\right] - k_g\,sat\left(\frac{s(t)}{\phi}\right). \quad (9)$$

where k_g is the gain, ϕ is the boundary layer thickness reducing the chattering of the control input, and "sat" is the saturation function. Also, the slave parameter estimations are considered inside the slave control law (represented with hat). Applying the control law in (9) to the slave dynamic and expressing in terms of s(t) gives

$$m_s\,\dot{s}(t) + \beta(t) + k_g\,sat\left(\frac{s(t)}{\phi}\right) = 0. \quad (10)$$

To satisfy the sliding condition, nonlinear gain k_g is given as

$$k_g \ge \eta.m_s + |\beta(t)|. \quad (11)$$

Where

$$\beta(t) = \left(b_s - \hat{b}_s\right)\dot{x}_s + \left(k_s - \hat{k}_s\right)x_s + \frac{\hat{m}_s - m_s}{\bar{m}_s}\left[\bar{b}_s\dot{x}_s + \bar{k}_s x_s + p\left(x_s - k_p\,\theta_m\right) + (1-\alpha)f_e\right]. \quad (12)$$

4. ROBUST CONTROLLER DESIGN

4.1 Fidelity

The controller in previous section result in the desired impedance equations (4) and (6). The linear relationship between inputs and outputs can be represented in hybrid matrix configuration. Using the Laplace notation, the hybrid matrix configuration is given as follows

$$H = \begin{bmatrix} \dfrac{\bar{J}_m s^2 + \bar{b}_m s + \bar{k}_m}{L_{eff}} & k_f \\ \dfrac{-k_p\,p}{\bar{m}_s s^2 + \bar{b}_s s + \bar{k}_s + p} & \dfrac{1-\alpha}{\bar{m}_s s^2 + \bar{b}_s s + \bar{k}_s + p} \end{bmatrix} \quad (13)$$

where

$$\begin{bmatrix} F_h \\ -X_s \end{bmatrix} = \overbrace{\begin{bmatrix} h_{11} & h_{12} \\ h_{21} & h_{22} \end{bmatrix}}^{H}\begin{bmatrix} \Theta_m \\ F_e \end{bmatrix} \quad (14)$$

Transparency is one of principal goals of teleoperation control system design. Transparency can be described quantitatively as a match between the environment impedance and the impedance transmitted to the operator. In applications such as robotic telesurgery it is important to improve the ability to detect compliance changes in the environment, which is called fidelity measure (Wang et al. 2005), in addition to the basic requirement of "good" tracking. Fidelity measure can be defined as

$$\mathcal{D}_z(Z_e) = \left\|\left(Z_t(s) - k_p\,k_f\,Z_{e0}(s)\right).l(s)\right\|_\infty \quad (15)$$

where Z_{e0} is the nominal environment impedance, Z_t is the impedance transmitted to the operator and $l(s)$ is a scalar low pass filter and is a weighting factor putting more emphasis on the lower frequencies. It also needs to be noted that the smaller the fidelity measure function value is, the better the performance of the system will be. Environment impedance transmitted through the teleoperation system can be expressed in terms of the hybrid matrix parameters as (Hashtrudi-Zaad et al. 2001)

$$Z_t(s) = \frac{f_h}{\theta_m} = h_{11} - \frac{h_{12}h_{21}Z_e}{1 + h_{22}Z_e} \quad (16)$$

The control design is formulated as an optimization problem to find the controller values which optimize the fidelity of the teleoperation system with constraints on stability and transparency (Wang et al. 2005). To minimize the fidelity measure, it is necessary to properly select two controller parameters in the hybrid matrix (p , α). The range value of these two gains were $p\epsilon[0 \quad 300]$ and $\alpha\epsilon[0 \quad 1]$.

4.2 Stability

Stability is the main goal of teleoperation control system design. In this study telemanipulation in soft environments was investigated. In stability inspection, a set of possible soft passive environment impedances were considered rather than all possible passive environment impedances. This decision was made to improve the fidelity as much as possible, due to the stability and performance trade off during control design. Moreover, the robust stability criterion is applied for multiplicative unstructured uncertainties as given in (Zhou and Doyle 1998).

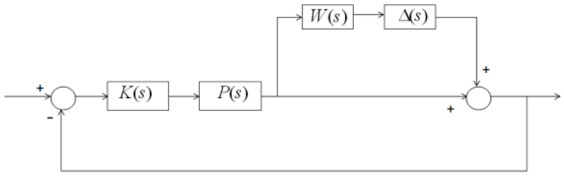

Fig. 1. A feedback system framework incorporated with multiplicative uncertainty

For a closed loop control system with multiplicative uncertainties as shown in Fig. 1, the following robust stability theorem is considered.

Theorem 1 (Robust stability condition)

Let $\prod = \{(I + W\Delta)P : \Delta\epsilon RH_\infty\}$ and let K be a stabilizing controller for the nominal plant P. Then the closed-loop system is well-posed and internally stable for all $\Delta\epsilon RH_\infty$ with $\|\Delta\|_\infty \le 1$ if and only if $\|TW\|_\infty \le 1$.

The complementation matrix T for the system is defined as follows

$$T = PK(I + PK)^{-1} \quad (17)$$

The uncertainty of the environment is considered. Once the range of the environment impedance uncertainty is determined, a constraint will be imposed on the controller parameters that can stabilize the system.

4.3 Position Tracking as a Constraint

The tracking requirement is necessary to prevent the final controller parameter optimization from yielding to a trivial solution. In addition, it is a fundamental performance requirement in telemanipulation systems (Cavusoglu et al. 2002). The free motion position tracking is used as a constraint. In free motion where environment force is zero, the transfer function from the reference input signal, $k_p x_m$, to the tracking error between the master and slave, $k_p x_m - x_s$, is the sensitivity function which can be obtained from hybrid matrix as follows

$$S_{en} = \frac{k_p\theta_m - x_s}{k_p\theta_m} = 1 + \frac{h_{21}}{k_p} = \frac{\bar{m}_s s^2 + \bar{b}_s s + \bar{k}_s}{\bar{m}_s s^2 + \bar{b}_s s + \bar{k}_s + p} \quad (18)$$

The input signal has been considered here is the scaled master position $k_p x_m$, which is a unit sinusoid signal with maximum frequency of 10 Hz and the output is the position tracking error between the master and slave. To keep this error less than 5%, the Bode plots for the transfer function S_{en} should be less than $20\,log(5\%) = -26.02dB$ for different values of p at the mentioned frequency range.

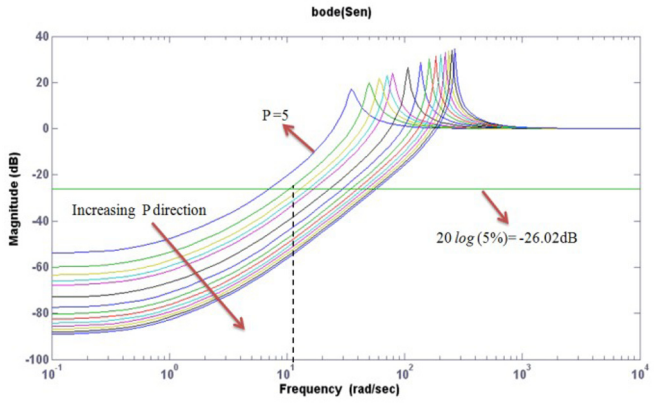

Fig. 2. S_{en} bode plot as a measure of tracking performance in free motion for several values for p

Generally, according to Fig. 2, the admissible limit for p is [15 300]. For example, as it is demonstrated in Fig. 2, for $p = 5$, the condition to minimize the error has been violated, where for example $p = 25$ has been suitably chosen to satisfy the condition.

4.4 Robust Stability and Fidelity Analysis

According to theorem 1, system stability in the nominal environment should be checked. For the teleoperation system, the loop gain $G(s)$ is calculated by Hannaford (1989) as

$$G(s) = \frac{-h_{12}h_{21}Z_e}{[h_{11} + Z_h][1 + h_{22}Z_e]}. \quad (19)$$

where h_{ij} for i,j=1,2 are the hybrid matrix entries. Z_e and Z_h are standing for environment and human impedances, respectively. The SISO closed-loop system is modelled in Fig. 3.

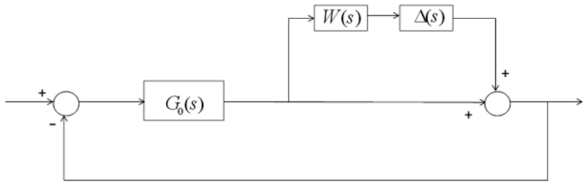

Fig. 3. Closed loop teleoperation system

Referring to Fig. 3, without considering the uncertainty term, the closed-loop transfer function can be obtained as

$$\hat{G}(s) = \frac{G_0(s)}{1 + G_0(s)}. \quad (20)$$

The nominal environment impedance is chosen to have a stiffness of $k_{e0} = 50\ N/m$. The range of environment stiffness is chosen as $Z_e = k_e\ \epsilon[10\ \ 150]\ N/m$. The range and nominal value of Z_e are experimentally determined from robotic needle insertion in chicken breast tissue with different insertion velocities.

The poles of the above transfer function for the nominal environment impedance Z_{e0} has been calculated. All the nominal closed loop systems are stable for $p\epsilon[60\ \ 300]$ and $\alpha\epsilon[0\ \ 1]$ because all poles belong to LHP.

To use theorem 1, multiplicative uncertainty weight for the system should be derived. The multiplicative uncertainty of the system can obtained as

$$G(s) = G_0(s)\big(1 + W(s)\Delta(s)\big)$$
$$= G_0(s).\left[\frac{1 + h_{22}(s)Z_{e0}(s)}{Z_{e0}(s)}.\frac{Z_e(s)}{1 + h_{22}(s)Z_e(s)}\right]. \quad (21)$$

$$W(s)\Delta(s) = \frac{Z_e(s) - Z_{e0}(s)}{Z_{e0}(s)}.\frac{1}{1 + h_{22}(s)Z_e(s)} \quad (22)$$

With the above equation, the upper bound of $W(s)$, $W_d(s)$, for the soft environment impedance range can be found which for all frequencies $W(s) < W_d(s)$. The set of uncertainty transfer functions for the environment impedance range and different values of p, α are shown in Fig. 4.

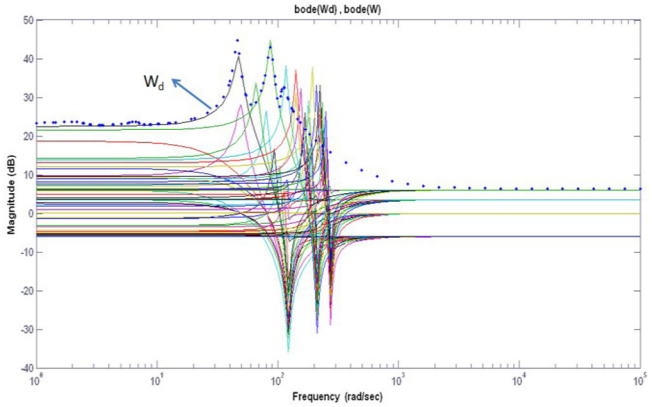

Fig.4. Environment uncertainty weighting functions, $W(s)$, and the upper bound $W_d(s)$ for the uncertainty.

The dotted curve on the top of the set of solid curves is the bounding function, which is calculated using Robust Control Toolbox of Matlab software.

The internal stability function $\|TW\|_\infty$ versus two control parameters is shown in Fig. 5 for $p\epsilon[60 \quad 300]$ and $\alpha\epsilon[0 \quad 1]$.

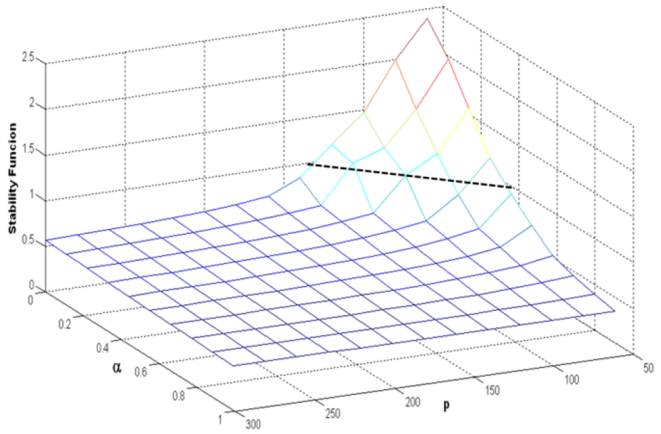

Fig. 5. Infinity norm of TW versus p and α as internal stability condition

As mentioned in theorem 1, when $\|\mathrm{TW}\|_\infty \leq 1$, the system is internally stable. As shown in Fig. 5, the theorem 1 requirement is not always satisfied. The bold line on the surface shows the contour of $\|\mathrm{TW}\|_\infty = 1$. Therefore the corresponding stability constraint on the controller parameters can be derived directly from Fig. 5.

Now, the parameter range that satisfies both stability and free motion tracking constraint are found. The next design step is to calculate the controller parameter values that minimize the fidelity function, $\mathcal{D}_z$. Using (15) and (16), the fidelity function value is depicted in Fig. 6 as a function of p and α.

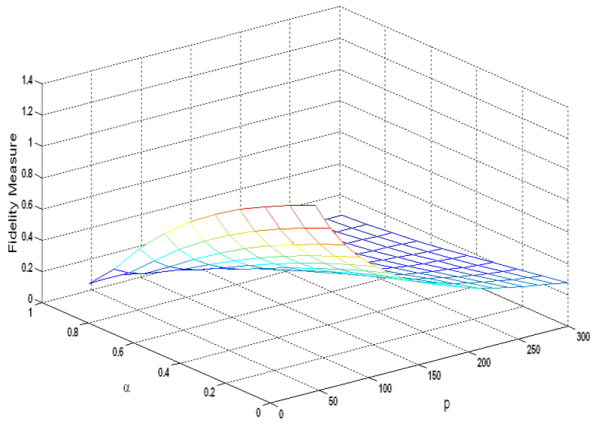

Fig. 6. Fidelity versus p and α as transparency measure

Now the optimum gain values are found that introduce the best fidelity. The best performance is available when the minimal fidelity function value $\mathcal{D}_z$ is achieved. The minimal fidelity function corresponds to $p = 300$ and $\alpha = 1$. Such a parameter pair can satisfy the robust stability constraint and free motion tracking constraint.

5. PARAMETER DESIGN

Parameters of communication channels, i.e. k_p and k_f, are chosen with respect to our specific manipulation task. Both impedance parameters of the master and slave controllers (i.e. $\bar{J}_m, \bar{b}_m, \bar{k}_m$ and $\bar{m}_s, \bar{b}_s, \bar{k}_s$) are designed to induce high dexterity to operator. Value of k_g is determined to satisfy (11) when the slave dynamic parameters are involved with uncertainty. ϕ is the smallest possible positive number which eliminates the unwanted chattering. All used parameters are listed in Table1.

Table1. Designed parameters

Symbol	Quantity(SI)	Symbol	Quantity(SI)	Symbol	Quantity(SI)
$\bar{J}_m$	0.001	$\bar{m}_s$	0.004	k_p	50/pi
$\bar{b}_m$	0.001	$\bar{b}_s$	0.02	k_f	3
$\bar{k}_m$	0.01	$\bar{k}_s$	0.01	ϕ	0.5

The overall block diagram of the teleoperation needle insertion system including master, slave and proposed controllers is shown in Fig. 7.

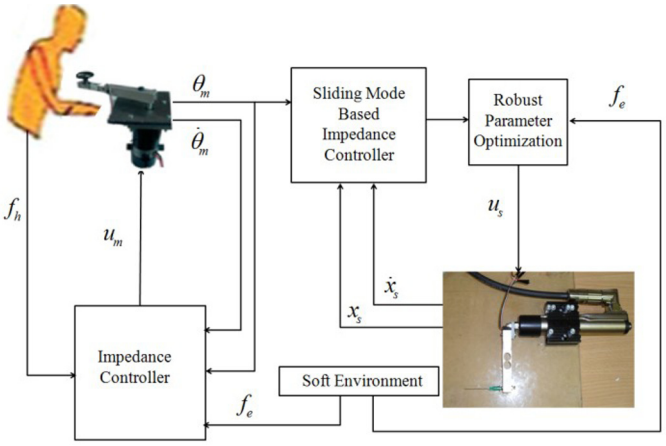

Fig.7.The overall block diagram of the teleoperation system

6. EXPERIMENTAL RESULT

In this section, the experimental results of the teleoperated needle insertion system are presented. A linear DC servo motor was used for insertion in soft tissues as the slave manipulator. The linear actuator type is P01−23×80 and is produced by Linmot Co. The motor encoder resolution is 1 micrometer and is driven by a B1100-GP driver. An 18 gauge bevel tip rigid needle was mounted on the motor. A high-precision load cell was used to measure the insertion force. The output of load cell was filtered using a low pass filter with a cutoff frequency of 100Hz to remove the force sensor noises. To test the proposed approach for soft environment, needle insertion tests were performed on a chicken breast tissue (Fig. 8). The master manipulator consisted of a DC servo-motor which was equipped with a high-resolution encoder. A load cell was installed on motor shaft to measure force exerted on the master (Fig. 9). An AX500 Digital Motor Controller was used for driving the DC servo-motor. A dSPACE data acquisition (DS1104) controller board was used as interface element between MATLAB Real-Time Workshop and the equipments. The controllers were

developed in Simulink and implemented in real time, using Matlab Real-Time Workshop, and through dSPACE Control Desk software. Force and position data were collected at a 1 kHz sample rate during needle insertion. For verification of the proposed controllers, the human operator manipulated the master end-effector to generate a desired position trajectory. The motion of the slave end-effector contains two stages as free motion and insertion stage.

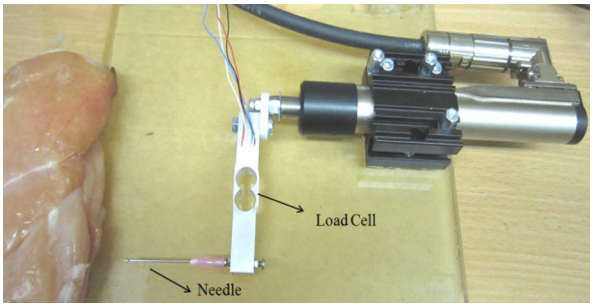

Fig. 8. Linear motor as the slave manipulator

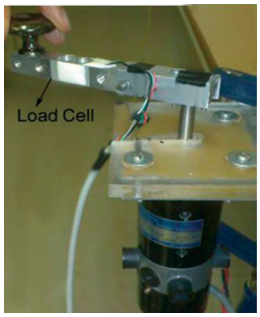

Fig. 9. The DC motor as the master manipulator

Fig. 10 shows the experimental results for position (10.a) and force (10.b) tracking. The proposed scheme shows good tracking performance. In spite of the contact with environment, the slave side can still track the master desired position while force reflected back to the master side is increasing. Fig. 10.b shows the variation of slave scaled force during needle insertion in the chicken breast. The controllers are capable of achieving both position and force tracking.

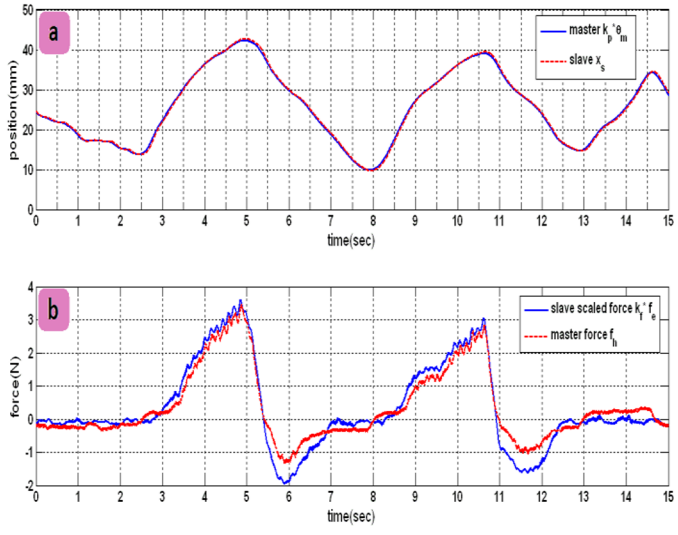

Fig. 10. Position and force tracking achieved in experiments

7. CONCOLUSIONS

In this research, a master/slave needle insertion was investigated and performed. The uncertainty of the slave and environment were taken into account, separately. The proposed sliding-mode controller at the slave side takes the slave uncertainty into consideration. Furthermore, an impedance controller for the master was implemented to achieve suitable force tracking. The proposed controllers make the teleoperation system robustly stable against parameter uncertainties. The control design was formulated as an optimization problem of finding the controller values which minimize the fidelity of the teleoperation system with constraints on stability and free motion tracking. The stability of the system under environment uncertainties was guaranteed by a modified robust controller. The experimental results verified the accurate position tracking in free motion and simultaneous position and force tracking during needle insertion. Briefly, a stable needle insertion was performed with high transparency.

REFRENCES

Abolhassani, N., Patel, R.V., Moallem, M. (2007). Needle insertion into soft tissue: a survey. *Medical Engineering and Physics*, **vol. 29**, pp. 413-431.

Abolhassani, N., Patel, R.V. (2009). Teleoperated master–slave needle insertion. *Medical Robotics and Computer Assisted Surgery* **vol. 5**, , pp. 398-405.

Buttolo, P., Braathern, P., Hannaford, B. (1994). Sliding control of force reflecting teleoperation: preliminary studies. *Presence*, **vol. 3**, pp.158-172.

Cavusoglu, M.C., Sherman, A., Tendick, F. (2002). Design of bilateral teleoperation controllers for haptic exploration and telemanipulation of soft environments. *IEEE transactions on robotics and automation*, **vol. 18**, pp. 641-647.

Cho, H.C., Park, J.H. (2005). Stable bilateral teleoperation under a time delay using a robust impedance control. *Elsevier journal of mechatronics*, **vol. 15**, pp. 611-625.

Hannaford, B. (1989). Stability and performance tradeoffs in bi-lateral telemanipulation. *IEEE International Conference on Robotics and Automation*, pp. 1764-1767.

Hashtrudi-Zaad, K., Salcudean, S.E. (2001). Analysis of control architectures for teleoperation systems with impedance/ admittance master and slave manipulators. *Journal of Robotics Research*, **vol. 20**, pp. 419-445.

Lu, Z., Goldenberg, A.A. (1995). Robust impedance control and force regulation: theory and experiments. *Journal of Robotics Research*, **vol. 14**, pp. 225-254.

Mahvash, M., Dupont, P.E. (2010). Mechanics of dynamic needle insertion into a biological material. *IEEE Transactions on Biomedical Engineering*, **vol. 57**, pp. 934-943.

Slotine, J.J.E., Li, W. (1991). Applied nonlinear control, pp.715-720, *Prentice-Hall*, Korea.

Wang, X., Liu, P.X., Wang, S. (2005). Adaptive robust control for bilateral teleoperators in soft environments. *IEEE Conference on Mechatronics & Automation*, pp. 2055-2060.

Zhou, K., Doyle, J.C. (1998). Essentials of robust control. *Prentice Hall*, Upper Saddle River, New Jersey, USA.